ELECTROMAGNETIC OPTIMAL DESIGN AND PREPARATION OF BROADBAND CERAMIC RADOME MATERIAL WITH GRADED POROUS STRUCTURE

F. Chen, Q. Shen, and L. Zhang

State Key Laboratory of Advanced Technology for Materials
Synthesis and Processing
Wuhan University of Technology
Wuhan 430070, China

Abstract—Silicon nitride (Si_3N_4) ceramic is a promising ultra-high speed (> 5 mach) broadband (1–18 GHz) radome material because of its excellent high-temperature resistance, good mechanical and dielectric properties. Si_3N_4 ceramics with A-sandwich wall structure are successfully applied to passive self-direction high transmission efficiency broadband radome (1–18 GHz). In the present study, a novel graded porous wall structure for broadband radome is promoted. The feasibility of using this structure is carried out by a computer aided design for the wall structure based on the microwave equivalent network method. By optimizing the layer number (n), structural coefficient (p), thickness (d) and dielectric constant (ε) of each layer, the power transmission efficiency at 1–18 GHz of graded porous Si_3N_4 ceramic radome is calculated. Si_3N_4 ceramics with graded porous structure are then prepared according to the design. The prepared sample exhibits a good graded porous structure with the porosity range from $\sim 2\%$ to 63 %. The tested power transmission efficiency at 1–18 GHz for the obtained sample matches well with the calculation results, indicating that the graded porous structure is feasible for the broadband radome application.

1. INTRODUCTION

A radome [1–3] acts as a protective cover to make the antenna inside work safely under abominable environment but does not interfere with its operation. Current missile development programs are endeavoring to increase both the flight speed (known as the Mach number) and the frequency bandwidth for guide control.

Corresponding author: Q. Shen (sqqf@263.net).

As shown in Fig. 1, the radome will suffer ultra-high temperature (1500–2000°C) when the missile flight speed is higher than 5 mach before hitting the target, which is a huge challenge for the radome material. As latest reported [4], silicon nitride (Si_3N_4) ceramic is the best candidate for the high speed radome application. Si_3N_4 has been used in numerous applications because of its superior properties, such as elevated high-temperature strength, good oxidation resistance and low thermal expansion coefficient [5–7]. Si_3N_4 has strong covalent chemical bond and two forms, α and β phases. Nowadays, various processing techniques have been developed to prepare both the porous and dense Si_3N_4 ceramics for structural and functional applications [8–12].
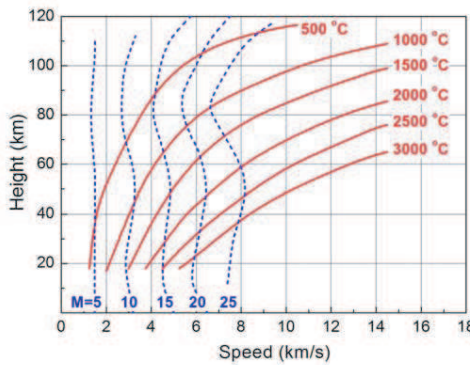

Figure 1. Missile flight speed as a function of the radome surface temperature and flight height.
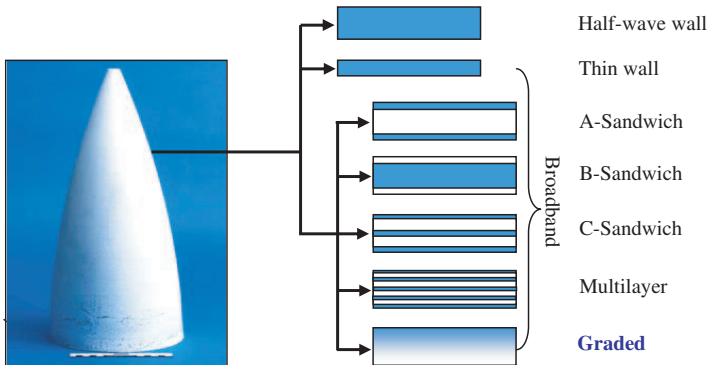

Figure 2. Schematic map of the radome wall structure.

The defined frequencies are often used for active or half-active self-direction missile system, while the broadband (such as $1 \sim 18\,\text{GHz}$) wave transmission efficient is often used for passive self-direction missile application, which is greatly determined by the radome wall structure [13, 14], as shown in Fig. 2. The traditional using half-wave wall structure is just for the defined frequency application [15]. The most commonly used and reported broadband radome wall structure includes A-sandwich, C-sandwich and multilayer. However, these structures are not suitable for high temperature environment, due to the big mismatch of the thermal properties of each layer (namely the ultra-high residual thermal stress), which may restrain their application in the high speed missile radome. Functionally graded materials (FGMs) have been developed early in the 1990s [16] and are considered to be one of the best structures to relax the thermal stress between layers, which are specially designed for ultra-high temperature application. Thus, we report on a novel structure, graded structure, for broadband and high speed passive self-direction radome application. Up to date, the graded porous structure with dense and porous layers has not been reported in the broadband radome application.

The purpose of this study is to investigate the feasibility of the graded porous structure for the broadband radome application by transmission efficiency calculation followed by optimizing the layer number (n), structural coefficient (p), thickness (d) and dielectric constant (ε) of each layer, and to explore the processing method for preparation of Si_3N_4 ceramics with graded porous structure. Finally, the transmission efficiency of the radome panel with graded porous structure is tested and compared with the numerical results.

2. OPTIMAL DESIGNS FOR THE RADOME WALL STRUCTURE

2.1. Hypotheses

Before designing a radome by calculating the transmission efficiency in an effective way, some hypotheses are made as follows:

(1) Plane wave solutions are used in mathematical descriptions of wave propagation in order to synthesis more complicated wavefronts. A plane wave is a mathematical but useful idealization because at large distances from sources and over regions of restricted size, curved wavefronts can be described approximately by plane wave functions.

(2) The theory of plane wave propagation through a plane dielectric sheet is used for radome design because a curved radome can be approximated as local plane. Thus, this paper studies propagation through flat sheets only. The flat sheet is a practically

useful and instructive boundary value problem, which demonstrates quantitatively how wave propagation depends on the dielectric constant and thickness of the sheet as well as the wave frequency, polarization, and incidence angle of the wave.

(3) A linearly polarized wave with the polarization either parallel or perpendicular to the plane of incidence is considered and the calculation methods for the complex valued transmission efficiency of a homogeneous, isotropic, nonmagnetic and dielectric sheet are developped.

2.2. Calculation Model

Over the past few decades, several simulation methods for broadband electromagnetic wave penetration property have been developed, including the basic electromagnetic wave theory, finite elemental analysis, transmission line method, etc [17–19]. For single layer structure, it is easy to calculate the wave transmission properties as described by Ref. [20]. For multilayer structure, such as A-sandwich (three layers), C-sandwich (five layers), etc., the calculation becomes complicated and it is difficult to calculate the transmission efficiency directly when the layer number is greater than five [21]. In the present study, a microwave equivalent network method is adopted to simplify the calculation for the graded porous structure. The calculation model
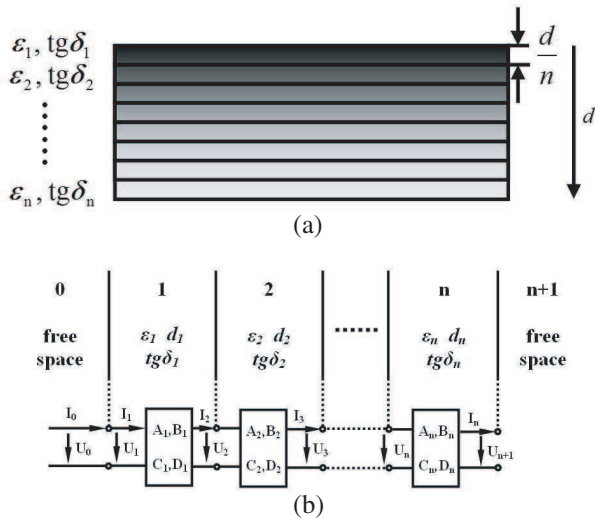

Figure 3. The calculation model of graded porous wall structure radome: (a) mathmatical model; (b) equivalent network model.
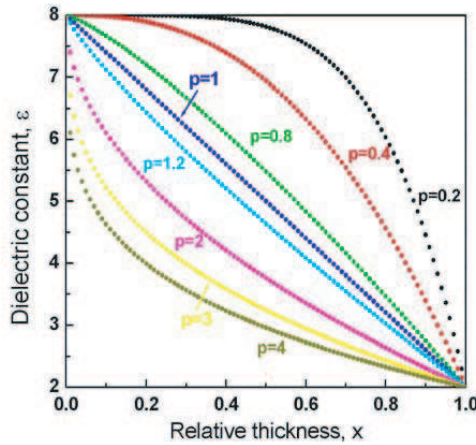
Figure 4. The dielectric constant (ε) of each layer as a function of the relative thickness (x) and structural coefficient (p) for graded porous structure.

of graded porous radome wall structure is shown in Fig. 3. The graded porous radome wall structure is divided into n layers with equal thickness and the thickness of each layer is d/n (d is the wall thickness). The top and the bottom layers stand for the outer and inner layer of the radome respectively. As a result, from the top to the bottom, porosity increases gradedly from 0 (fully dense) to the highest value, while the dielectric constant decreases from the highest value ε_1 to the lowest value ε_n. Thus, the dielectric constant of each layer can be expressed by Eq. (1).

$$\varepsilon = \varepsilon_n + (\varepsilon_1 - \varepsilon_n)(1 - (x)^{1/p}) \qquad (1)$$

where x is the relative thickness, and p is the structural coefficient of the graded porous radome material. The dielectric constant (ε) of each layer as a function of the relative thickness (x) and structural coefficient (p) is calculated and shown in Fig. 4. It is illustrated in Fig. 4 that the greater the p is, the higher the relative thickness of layer containing the low dielectric constant material is, which is severe to the mechanical reliability for the radome. As a result, a low p value is expected in the design for the broadband radome. And $p = 4$ is selected as the initial condition for the following calculation.

Figure 3(b) is the microwave equivalent network map for the model shown in Fig. 3(a). Thus, it is easy to calculate the transmission efficiency by using the fundamental matrix of the transmission line

model, which is expressed by Eq. (2).

$$
\begin{bmatrix} \mathbf{A} & \mathbf{B} \\ \mathbf{C} & \mathbf{D} \end{bmatrix} = \begin{bmatrix} \cos \mathbf{k_1 d_1} & j\frac{\mathbf{Z_1}}{\mathbf{Z_0}} \sin \mathbf{k_1 d_1} \\ j\frac{\mathbf{Z_0}}{\mathbf{Z_1}} \sin \mathbf{k_1 d_1} & \cos \mathbf{k_1 d_1} \end{bmatrix} \cdot \begin{bmatrix} \cos \mathbf{k_2 d_2} & j\frac{\mathbf{Z_2}}{\mathbf{Z_0}} \sin \mathbf{k_2 d_2} \\ j\frac{\mathbf{Z_0}}{\mathbf{Z_2}} \sin \mathbf{k_2 d_2} & \cos \mathbf{k_2 d_2} \end{bmatrix}
$$
$$
\cdots \begin{bmatrix} \cos \mathbf{k_n d_n} & j\frac{\mathbf{Z_n}}{\mathbf{Z_0}} \sin \mathbf{k_n d_n} \\ j\frac{\mathbf{Z_0}}{\mathbf{Z_n}} \sin \mathbf{k_n d_n} & \cos \mathbf{k_n d_n} \end{bmatrix} \tag{2}
$$

where $k_n = \frac{2\pi}{\lambda_0}\sqrt{\dot{\varepsilon}_n - \sin^2 \theta_0}$, $\dot{\varepsilon}_n = \varepsilon_n(1 - j\mathrm{tg}\delta_n)$, and d is the wall thickness, λ_0 is the incident wavelength, and θ_0 is the incidence angle, Z is the electromagnetic wave impedance.

The calculation of Z for perpendicular polarization is given by Eq. (3).

$$
\frac{Z_n}{Z_0} = \frac{\sqrt{\dot{\varepsilon}_n - \sin^2 \theta_0}}{\dot{\varepsilon}_n \cos \theta_0} \tag{3}
$$

while calculation of Z for parallel polarization is given by Eq. (4).

$$
\frac{Z_n}{Z_0} = \frac{\cos \theta_0}{\sqrt{\dot{\varepsilon}_n - \sin^2 \theta_0}} \tag{4}
$$

From Eqs. (3) and (4), it is clearly seen that when $\theta_0 = 0$, The Z of perpendicular polarization is equal to that of parallel polarization. In order to simplify the calculation, we use $\theta_0 = 0$ in the following calculations and materials power transmission efficiency test.

The power transmission efficiency is $|T|^2$, where T is given by Eq. (5).

$$
T = \frac{2}{A + B + C + D} \tag{5}
$$

3. NUMERICAL RESULTS AND DISCUSSION

For the calculation of power transmission efficiency of graded porous structure, the effect of layer number (n), structural coefficient (p), wall thickness (d), dielectric constant of inner layer (ε_n) and outer layer (ε_n) should be taken into consideration. Based on the Si_3N_4 ceramic which is selected as the radome material in the present paper, the dielectric constant of as-prepared dense Si_3N_4 ceramic is ~ 8, while dielectric constant of the as-prepared porous Si_3N_4 ceramic with highest porosity is ~ 2. Meanwhile, Si_3N_4 ceramic radome wall thickness is evaluated in Ref. [22], based on their design results, wall thickness of $d = 6\,\mathrm{mm}$ is selected.
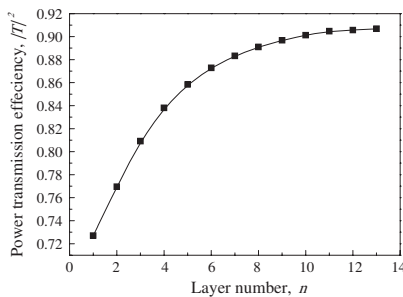
3.1. Effect of Layer Number (n) on the Transmission Efficiency of the Graded Radome Material

The initial conditions are: $p = 4$, $d = 6\,\text{mm}$, $\varepsilon_n = 2$ and $\varepsilon_1 = 8$.

The transmission efficiency of the graded porous panel as functions of the frequency and layer number (n) is shown in Fig. 5(a). It is obviously seen that the greater the n is, the higher the broadband transmission efficiency is, indicating that the continuous gradient structure has better power transmission efficiency than the multilayer gradient structure. When $n > 5$, the power transmission efficiency is higher than 70% at 1–18 GHz, which is good for the missile guide control. On the other hand, the transmission efficiency as a function of the layer number (n) at 10 GHz is shown in Fig. 5(b). It is obviously seen that when n is less than 5, the transmission efficiency increases greatly with the increase of n, but it fluctuates little when n is greater than 5. Thus, the layer number $n = 5$ will be more feasible for the preparation of the gradient porous structure Si_3N_4 ceramic radome material. However, in order to precisely calculate the transmission efficiency, we choose $n = 10$ in the following calculations.
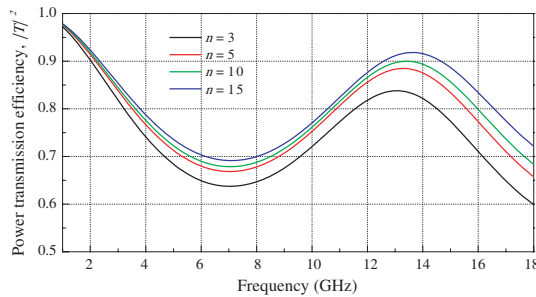
Figure 5. Power transmission efficiency of the graded panel material as functions of frequency and layer number.
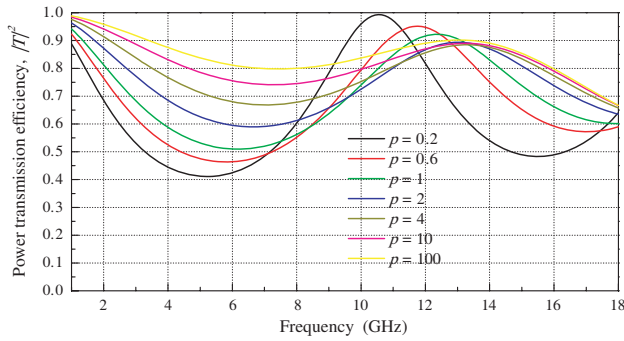
Figure 6. Power transmission efficiency of the graded panel material as functions of frequency and structural coefficient.

3.2. Effect of Structural Coefficient (p) on the Transmission Efficiency of the Graded Radome Material

The initial conditions are: $n = 10$, $d = 6$ mm, $\varepsilon_n = 2$ and $\varepsilon_1 = 8$.

The transmission efficiency of the graded porous panel as functions of the frequency and structural coefficient (p) is shown in Fig. 6. According to Fig. 6, it is seen that the greater the p is, the higher the broadband transmission efficiency is. It is also observed that p plays a very important role in the single frequency application. For example, at frequency of 10.5 GHz, $p = 0.2$ is the best choice with transmission efficiency is close to 100%, while at frequency of 12 GHz, $p = 0.6$ is the best. As a low p value is expected in the design for the broadband radome, for broadband application at 1–18 GHz, it is seen that the transmission efficiency shows nearly no difference in the frequency range of 13–18 GHz when p is 4 or higher. Also when p is 4 or higher, the transmission efficiency at 1–13 GHz is higher than 70%, which can be practically used. Thus, we choose $p = 4$ in the following calculation and preparation of the graded radome material.

3.3. Effect of Wall Thickness (d) on the Transmission Efficiency of the Graded Radome Material

The initial conditions are: $n = 10$, $p = 4$, $\varepsilon_n = 2$ and $\varepsilon_1 = 8$.

The transmission efficiency of the gradient porous panel as functions of the frequency and wall thickness (d) is shown in Fig. 7. According to Fig. 7, it is seen that when d is less than 10 mm, the transmission efficiency shows almost no difference, and when d is less than 7 mm, the transmission efficiency is higher than 70%, which fulfills the requirements for the broadband radome application and

has a similar conclusion with Ref. [23]. Specially, if the radome is used at defined frequency, the thickness can be selected by the applied frequencies and the mechanical properties. Considering the mechanical requirements for the broadband radome, a certain thickness is needed. As a result, we choose $d = 6\,\mathrm{mm}$ in the preparation of Si_3N_4 gradient ceramic radome material, after considering both the broadband transmission property and the mechanical property.

3.4. Effect of Dielectric Constant (ε) on the Transmission Efficiency of the Graded Radome Material

The initial conditions are: $n = 10$, $p = 4$, $d = 6\,\mathrm{mm}$, $\varepsilon_n = 2$ and $\varepsilon_1 = 8$.
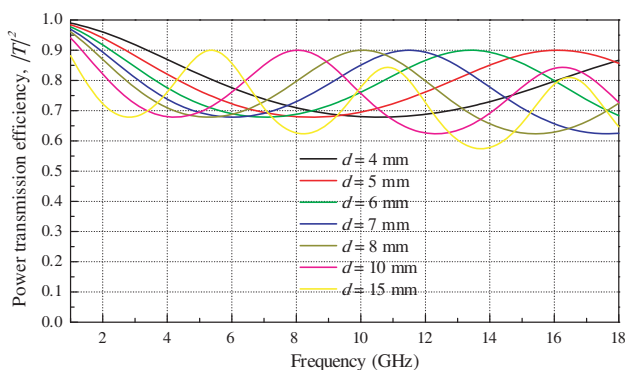

Figure 7. Power transmission efficiency of the graded panel material as functions of frequency and wall thickness.
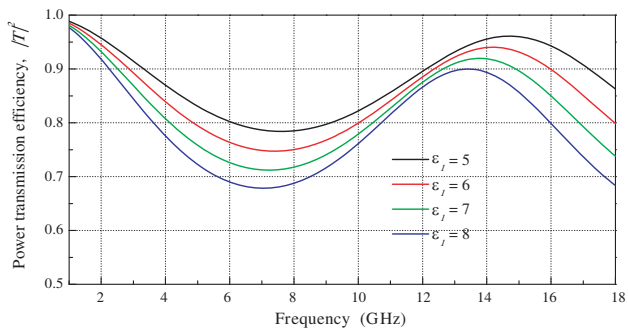

Figure 8. Power transmission efficiency of the graded panel material as functions of frequency and dielectric constant of outer layer.
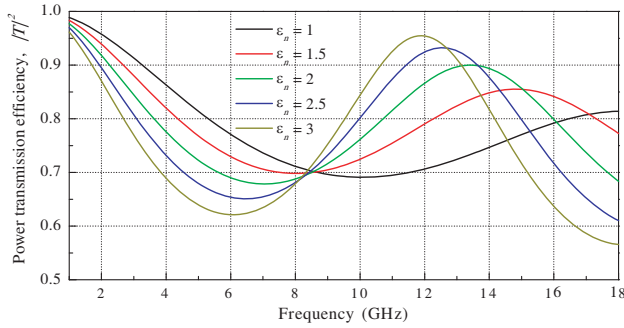
Figure 9. Transmission efficiency of the porous graded panel as functions of frequency and ε_n.

The transmission efficiency of the graded panel material as functions of the frequency and dielectric constant of outer layer (ε_1) is shown in Fig. 8. It is obviously seen that the transmission efficiency decreases with the increase of ε_1. Our previous experiment suggested that when MgO and $AlPO_4$ are used as the sintering additives, the dielectric constant for the fully dense sample is ~ 7. In this situation, according to Fig. 8, the transmission efficiency is higher than 75%, which fulfills the requirements for the broadband radome application.

On the other hand, the transmission efficiency of the graded panel material as functions of the frequency and dielectric constant of inner layer (ε_n) is shown in Fig. 9. It is obviously seen that the transmission efficiency decreases with the increase of ε_n. When ε_n is less than 2.5, the transmission efficiency is higher than 75%, which fulfills the requirements for the broadband radome application.

From the above calculations, the as-designed conditions for the preparation of the Si_3N_4 broadband ceramic radome material are: $n = 5$, $p = 4$, $d = 6\,\text{mm}$, $\varepsilon_n < 2.5$ and $\varepsilon_1 < 8$.

4. EXPERIMENTAL PROCEDURES

Considering the optimal design results, according to our experimental progress in the past years, the material used for the preparation of the graded porous Si_3N_4 ceramic has been selected. Firstly, Si_3N_4 ceramics with nearly fully dense have been prepared by using MgO and $AlPO_4$ as the sintering additive and spark plasma sintering technique, the dielectric constant of which is ~ 7.0 [24]. This material has actual the lowest porosity and the maximum dielectric constant, and is used as the "top" layer for the preparation of the graded porous Si_3N_4
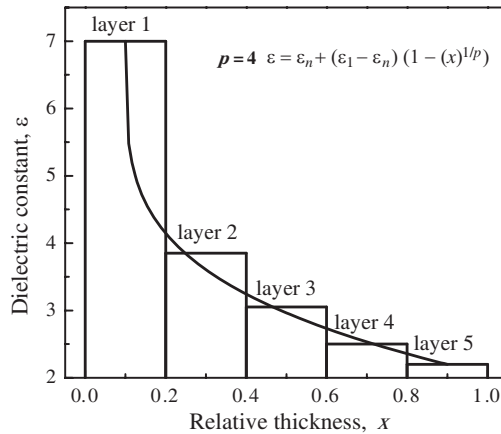
Figure 10. The dielectric constant of each layer for a 5 layers graded porous ceramic design when $\varepsilon_1 = 7$ and $\varepsilon_n = 2.2$.

ceramics. Secondly, several methods have been applied to prepare Si_3N_4 porous ceramics with high porosity and low dielectric constant. The sample using 50 vol.% H_3PO_4 as the pore-forming agent is tested to have the highest porosity ($\sim 63\%$) and the lowest dielectric constant ($\varepsilon_n = 2.2$) [25]. Thus, in terms of Eq. (1), for 5 layers porous graded ceramics, the dielectric constant of each layer when $p = 4$ is shown in Fig. 10. As a result, the dielectric constant for the other three layers can be calculated for the experimental design.

The raw materials used in the present study are as follows: commercial fine Si_3N_4 powder whose particle shape is sphere, average grain size is $\sim 0.5\,\mu m$ and the content of α phase is higher than 93%; commercial zirconia (ZrO_2) powder whose grain size is $\sim 0.5\,\mu m$ and the purity is up to 99.9%; commercial magnesia (MgO) and alumina phosphate ($AlPO_4$) powder whose grain size is $< 0.2\,\mu m$ and the purity was up to 99.9% and phosphorus acid (H_3PO_4) liquid whose concentration is 85% and the purity is up to 99.9%.

Graded porous Si_3N_4 ceramic with 5 layers is prepared by stacking orderly the 5 individual prepared Si_3N_4 ceramics, using a phosphate binder by thermally treated at $200°C$. The preparation method for the dense and porous Si_3N_4 ceramics have been published and presented in detail in the Refs. [24–26]. The physical properties and the composition of each layer of porous graded Si_3N_4 ceramics are listed in Table 1.

After sintering, the microstructure of the fractured surfaces is observed by scanning electron microscopy (SEM). The dielectric constant and dielectric loss of bulk samples is tested at frequency of

Table 1. Composition and physical properties of each layer of the graded porous Si_3N_4 ceramics.

N	Composition and preparation method	d (mm)	Porosity (%)	ε	tgδ
1	$Si_3N_4 + 4$ wt.% $MgO + 16$ wt.% $AlPO_4$ (Spark plasma sintering, 1400°C, 5 min)	1.2	< 2	7.0	0.006
2	$Si_3N_4 + 20$ wt.% ZrP_2O_7 (Pressureless sintering, 1000°C, 2 h)	1.2	~ 40	3.8	0.006
3	$Si_3N_4 + 35$ vol.% H_3PO_4 (Pressureless sintering, 1000°C, 2 h)	1.2	~ 46	3.0	0.005
4	$Si_3N_4 + 40$ vol.% H_3PO_4 (Pressureless sintering, 1000°C, 2 h)	1.2	~ 55	2.5	0.006
5	$Si_3N_4 + 50$ vol.% H_3PO_4 (Pressureless sintering, 1000°C, 2 h)	1.2	~ 63	2.2	0.002

10 GHz, according to method reported in [27]. The power transmission efficiency of the graded panel sheet with the size of 100×100 mm is tested by free space transmission method in a dark microwave room, which is similar to the method in Refs. [28, 29]. It consists of a network analyzer where the incident and transmission ports are connected to two horn antennas located on each side of the test panel. The test includes two steps: firstly, data (1) are collected without the ceramic radome panel; then, data (2) are collected when the ceramic radome panel is set. And the transmission efficient is calculated by using data (1) and (2). For broadband transmission efficient test, we have to change the antenna for several times, according to different frequencies used. The test frequency is 1–18 GHz.

5. EXPERIMENTAL RESULTS AND DISCUSSION

SEM image of the obtained Si_3N_4 ceramic with graded porous structure is illustrated in Fig. 11. From this image, it is observed obviously that the pores are increased gradually from layer 1 to layer 5, indicating that an expected graded porous structure Si_3N_4 ceramic is successfully prepared by the present technique. On the other hand, the pore size can be well controlled and increased gradually from less than 0.5 μm to several μm, suggesting that the obtained graded porous Si_3N_4 ceramic may have promising mechanical and thermal matching property. Generally, a large amount of fine and uniform open

micropores are observed from layer 2 to layer 5. Moreover, the Si_3N_4 grains are fine and maintained almost the same particle size of the raw Si_3N_4 powder. For each individual layer, it is isotropic structure, and the anisotropic effect for each individual layer is considered to be very limited. As a result, the obtained Si_3N_4 ceramic with porous graded structure is quite in agreement with the design model as shown in Fig. 3. Thus, it is easy to adjust and improve the experimental conditions to prepare the graded structure with various layers, porosities (namely dielectric constant), layer thickness, etc., according to the electromagnetic microwave calculation and design.

Both calculation value and tested value of the power transmission efficiency of the graded porous structure Si_3N_4 ceramic radome panel at the incident angle of zero is shown in Fig. 12. It is seen that the tested transmission efficiency is higher than 75% at the frequency range of 1–18 GHz, indicating that the graded porous structure has an ideal broadband transmission property. It is feasible to use
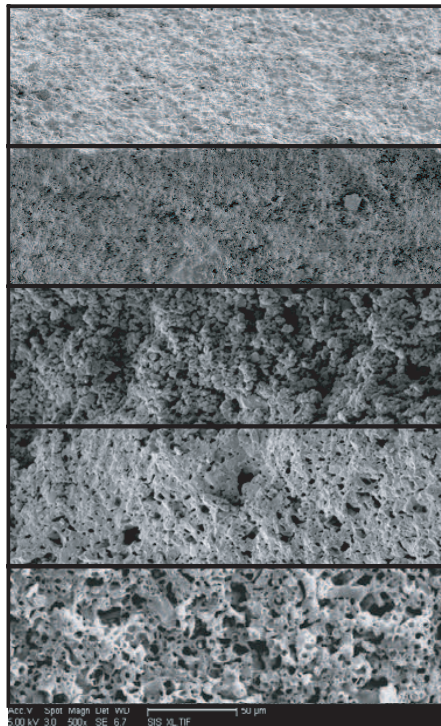

Figure 11. SEM image of the obtained Si_3N_4 ceramic with graded porous structure.
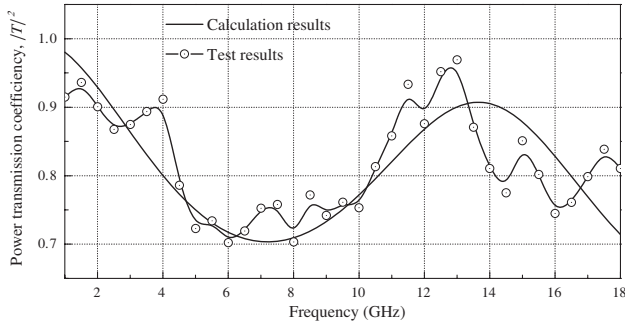
Figure 12. The calculation value and tested value of power transmission efficiency of the graded porous structure Si_3N_4 ceramic radome panel at the incident angle of zero.

the graded porous structure for the broadband radome application. Compared with the calculation results obtained by using the same physical properties and structural parameters with the experiment, it is clearly seen that the two are nearly in agreement with each other, suggesting that the electromagnetic microwave transmission calculation and optimal design are essential and play a significant role before the experiment being carried out. The reason for the differences between the experiment and simulation is that the microwave equivalent network method used is not accurate enough to be stand alone tool. Moreover, the effect of temperature and curvature shape on the transmission efficiency needs further investigation for the graded porous structure radome application.

6. CONCLUSION

1. Calculation model of graded porous wall structure is established, the microwave equivalent network method is used for transmission efficiency calculation. When the initial conditions are $n = 5$, $p = 4$, $d = 6$ mm, $\varepsilon_n < 2.5$ and $\varepsilon_1 < 8$, the power transmission efficiency is higher than 70% at frequency range of 1–18 GHz, suggesting that graded structure is feasible in broadband radome application.

2. A five layer graded porous Si_3N_4 ceramic radome material is prepared according to the experimental design.

3. The tested power transmission efficiency of the prepared graded porous Si_3N_4 ceramic radome material is higher than 75% at the frequency range of 1–18 GHz and is in agreement with the calculation results.

ACKNOWLEDGMENT

REFERENCES

1. Persson, K., M. Gustafsson, and G. Kristensson, "Reconstruction and visualization of equivalent currents on a radome using an integral representation formulation," *Progress In Electromagnetics Research B*, Vol. 20, 65–90, 2008.

2. Sukharevsky, O. I. and V. A. Vasilets, "Scattering of reflector antenna with conic dielectric radome," *Progress In Electromagnetics Research B*, Vol. 4, 159–169, 2008.

3. Persson, K. and M. Gustafsson, "Reconstruction of equivalent currents using a near-field data transformation — With radome applications," *Progress In Electromagnetics Research*, PIER 54, 179–198, 2005.

4. Ceramic Radomes for Tactical Missile Systems, www.ceradyne-thermo.com.

5. Shen, Z. J., Z. Zhao, H. Peng, et al., "Formation of tough interlockingmicrostructures in silicon nitrideceramics by dynamic ripening," *Nature*, Vol. 417, 266–269, 2002.

6. Peterson, I. M. and T. Y. Tien, "Effect of the grain boundary thermal expansion coefficient on the fracture toughness in silicon nitride," *J. Am. Ceram. Soc.*, Vol. 78, No. 9, 2345–2352, 1995.

7. Riley, F. L., "Silicon nitride and related materials," *J. Am. Ceram. Soc.*, Vol. 83, No. 2, 245–265, 2000.

8. Pyzik, A. J. and D. R. Beaman, "Microstructure and properties of self-reinforced silicon nitride," *J. Am. Ceram. Soc.*, Vol. 76, No. 11, 2737–2744, 1993.

9. Diaz, A., S. Hampshire, J. F. Yang, T. Ohji, and S. Kanzaki, "Comparison of mechanical properties of silicon nitrides with controlled porosities produced by different fabrication routes," *J. Am. Ceram. Soc.*, Vol. 88, No. 3, 698–706, 2005.

10. Shan, S. Y., J. F. Yang, J. Q. Gao, W. H. Zhang, and Z. H. Jin, "Porous silicon nitride ceramics prepared by reduction–nitridation of silica," *J. Am. Ceram. Soc.*, Vol. 88, No. 9, 2594–2596, 2005.

11. Kawai, C. and A. Yamakawa, "Effect of porosity and microstructure on the strength of Si_3N_4: Designed microstructure for high strength, high thermal shock resistance, and facile machining," *J. Am. Ceram. Soc.*, Vol. 80, No. 10, 2705–2708, 1997.

12. Lam, D. C. C., F. F. Lange, and A. G. Evans, "Mechanical properties of partially dense alumina produced from powder compacts," *J. Am. Ceram. Soc.*, Vol. 77, No. 8, 2113–2117, 1994.

13. Nie, X.-C., N. Yuan, L.-W. Li, T. S. Yeo, and Y.-B. Gan, "Fast analysis of electromagnetic transmission through arbitrarily shaped airborne radomes using precorrected-FFT method," *Progress In Electromagnetics Research*, PIER 54, 37–59, 2005.

14. Paris, D. T., "Computer-aided radome analysis," *IEEE Trans. Antennas and Propag.*, Vol. 18, No. 1, 7–15, January 1970.

15. Gu, J., Y. Fan, Y. H. Zhang, and D. K. Wu, "Novel 3-D half-mode SICC resonator for microwave and millimeter-wave applications," *Journal of Electromagnetic Waves and Applications*, Vol. 23, No. 11–12, 1429–1439, 2009.

16. Mortensen, A. and S. Suresh, "Functionally graded metals and metal-ceramic composites. 1. Processing," *Int. Mater. Rev.*, Vol. 40, No. 6, 239–265, 1995.

17. Hasar, U. C., O. Simsek, and M. Gulnahar, "Simple procedure to simultaneously evaluate the thickness of and resistive losses in transmission lines from uncalibrated scattering parameter measurements," *Journal of Electromagnetic Waves and Applications*, Vol. 23, No. 8–9, 999–1010, 2009.

18. Kedar, A. and U. K. Revankar, "Parametric study of flat sandwich multilayer radome," *Progress In Electromagnetics Research*, PIER 66, 253–265, 2006.

19. Kedar, A., K. S. Beenamole, and U. K. Revankar, "Performance appraisal of active phased array antenna in presence of a multilayer flat sandwich radome," *Progress In Electromagnetics Research*, PIER 66, 157–171, 2006.

20. Kong, J. A., *Electromagnetic Wave Theory*, Wiley-Interscience, May 2008.

21. Fuerholz, P. and A. Murk, "Design of a broadband transition using the constant impedance structure approach," *Progress In Electromagnetics Research Letter*, Vol. 7, 69–78, 2009.

22. Kozakoff, D. J., *Analysis of Radome Enclosed Antennas*, Artech House, Norwood, MA, 1997.

23. Sunil, S., K. S. Venu, S. M. Vaitheeswaran, and U. Raveendranath, "A modified expression for determining the wall thickness of

monolithic half-wave radomes," *Microw. Opt. Techn. Lett.*, Vol. 30, No. 5, 350–352, 2001.

24. Chen, F., Q. Shen, F. Q. Yan, and L. M. Zhang, "Spark plasma sintering of α-Si$_3$N$_4$ ceramics with MgO-AlPO$_4$ as sintering additives," *Mater. Chem. Phys.*, Vol. 107, 67–71, 2008.

25. Chen, F., Q. Shen, F. Q. Yan, and L. M. Zhang, "Pressureless sintering of α-Si$_3$N$_4$ porous ceramics using H$_3$PO$_4$ pore-forming agent," *J. Am. Ceram. Soc.*, Vol. 90, No. 8, 2379–2383, 2007.

26. Chen, F., Q. Shen, F. Q. Yan, and L. M. Zhang, "Preparation of zirconium pyrophosphate bonded silicon nitride porous ceramics," *Mater. Sci. Technol.*, Vol. 22, No. 8, 915–918, 2006.

27. Chou, Y. H., M. J. Jeng, Y. H. Lee, and Y. G. Jan, "Measurement of RF PCB dielectric properties and losses," *Progress In Electromagnetics Research Letter*, Vol. 4, 139–148, 2008.

28. Audone, B., A. Delogu, and P. Morindo, "Radome design and measurements," *IEEE Trans. Instrument. Measure.*, Vol. 37, No. 2, 292–295, 1988.

29. Meng, H. F. and W. B. Dou, "A hybrid method for the analysis of radome-enclosed horn antenna," *Progress In Electromagnetics Research*, PIER 90, 219–233, 2009.